18 February 2000

ELSEVIER

Chemical Physics Letters 318 (2000) 53–57

CHEMICAL PHYSICS LETTERS

www.elsevier.nl/locate/cplett

Studies of nonlinear absorption and refraction in C_{60}/toluene solution

Tai-Huei Wei [a,*], Tzer-Hsiang Huang [a], Tzung-Tao Wu [a], Pei-Chang Tsai [a], Mu-Shih Lin [b]

[a] *Department of Physics, National Chung-Cheng University, Ming-Hsiung, Chia-Yi, Taiwan, ROC*
[b] *Department of Applied Chemistry, National Chiao-Tung University, Hsinchu, Taiwan, ROC*

Received 27 August 1999

Abstract

Nonlinear absorptive and refractive properties of C_{60}/toluene solution are studied using the *Z*-scan technique and a 532 nm laser delivering single picosecond (ps) pulses and trains of ps pulses separated by 7 nanoseconds (ns). With single ps pulses, reverse saturable absorption and positive nonlinear refraction are observed and attributed to population transitions among the singlet states. With ps pulse trains, a sign change of nonlinear refraction relative to that of single ps-pulse excitation is observed and is attributed to heat-induced temperature rise and population relaxing to triplet states.

1. Introduction

Optical materials with large coefficients of reverse saturable absorption (RSA) and nonlinear refraction can exhibit irradiance-dependent transmittance (transmitted energy/input energy) and phase shift, which cooperatively limit the throughput fluence (optical energy per unit of area). Such materials are of prime importance in optical limiting related applications [1]. The fullerene molecules have attracted much attention recently because, as three-dimensional π-electron conjugated systems, they appear promising as new limiting materials [2]. In this Letter we report the results of our *Z*-scan investigation on the fullerene C_{60} dissolved in toluene. Particularly, we use a five-state model to explain the observed RSA in the picosecond (ps) regime as well as to distinguish the mechanisms that contribute to ps and nanosecond (ns) nonlinear refraction, which show opposite signs when the coexistent nonlinear absorption is eliminated.

2. Experimental method

The *Z*-scan technique is a single beam method for measuring both nonlinear absorption and nonlinear refraction. Its operation, as shown in the inset of Fig. 1, involves measurements of the far field sample

* Corresponding author. Fax: +886-5-272-0587; e-mail: twei@phy.ccu.edu.tw

0009-2614/00/$ - see front matter
PII: S0009-2614(00)00011-7

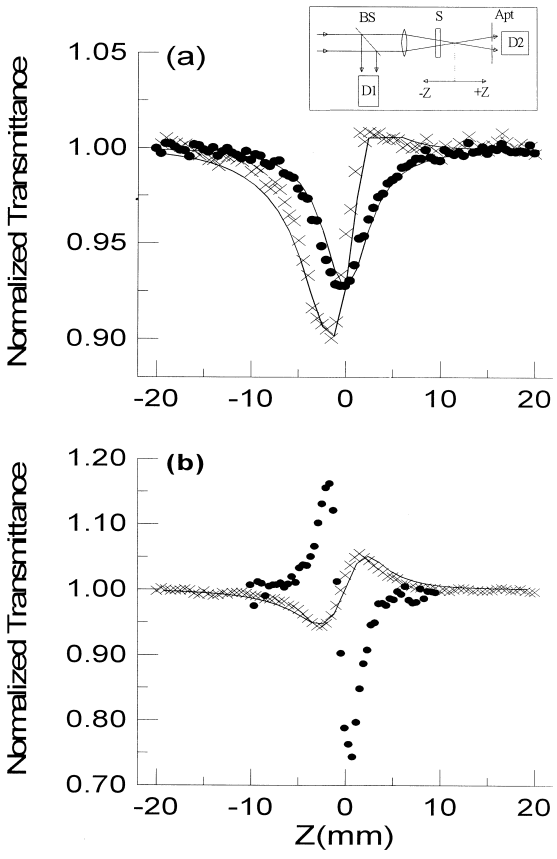

Fig. 1. (a) The *Z*-scan results of C_{60}/toluene solution using single ps pulses. Crosses: with an aperture; dots: without aperture; solid lines: theoretical. (b) The divided *Z*-scan curve of C_{60}/toluene using ps pulses (crosses) and the full pulse envelopes (dots). The solid line is the theoretical fit to the crosses. Inset: The *Z*-scan apparatus in which the ratio D_2/D_1 is recorded as a function of the sample position (z).

transmittance (transmitted energy detected by D_2 divided by input energy monitored by D_1) of a focused Gaussian beam as a function of the sample position (z) relative to the beam waist [1]. An aperture is optionally placed in front of D_2. When the aperture is absent, total transmitted energy is detected, and the resultant *Z*-scan curve reveals nonlinear absorption alone. When the aperture is present, beam distortion (broadening or narrowing) induced by nonlinear phase shift, in addition to nonlinear absorption, affects the amount of energy through the aperture. The result thus contains both nonlinear absorption and nonlinear refraction. Division of the *Z*-scan curve obtained with an aperture by that without aperture yields a curve with nonlinear absorption effectively eliminated. This curve, referred to as the divided *Z*-scan curve, reveals the effect of nonlinear refraction alone [1].

In this study, we use a Q-switched and mode-locked Nd:YAG laser for both the ps and ns investigations. This laser is frequency doubled to give an output wavelength of $\lambda = 532$ nm and operated in the TEM_{00} mode with a half-width at e^{-2} irradiance at focus of $\omega_0 = 21$ μm. For the ns nonlinearity investigation, we use the full output envelopes containing eleven 19 ps (HW1/eM) pulses separated by 7 ns (Fig. 2, top). For the ps nonlinearity investigation, we use the single ps pulses switched out of the envelopes (Fig. 2, bottom) by a Pockels cell sandwiched between two crossed polarizers.

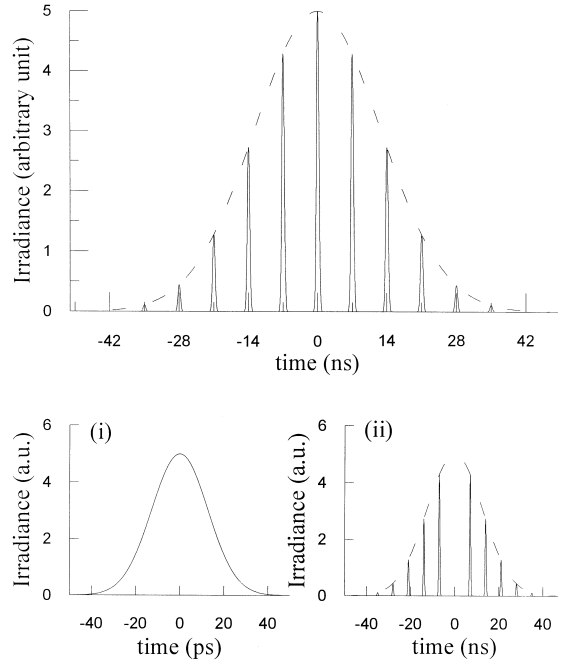

Fig. 2. Top: the temporal profile of the full pulse envelope. Bottom: (i) the single ps pulse switched out of the full pulse envelope; and (ii) the extraction (missing) of the single ps pulse from the pulse envelope.

The irradiance and phase of a switched-out single ps pulse, incident on the sample at z, can be written as [3]

$$I_0 = I(z, r, t) = \left[\frac{\omega_0^2}{\omega^2(z)}\right] I_{00} \exp\left[-\frac{2r^2}{\omega^2(z)}\right] \times \exp\left[-\left(\frac{t}{\tau}\right)^2\right] \quad (1)$$

and

$$\phi_0 = \phi(z, r) = \frac{kr^2}{2R(z)}. \quad (2)$$

In Eq. (1), the origin of time is set at the pulse maximum; the argument r refers to the lateral distribution of the laser beam. $\omega(z) = \omega_0[1 + (z/z_0)^2]^{1/2}$ is the beam radius at z, $R(z) = z[1 + (z_0/z)^2]$ is the curvature radius of the wave front at z, $z_0 = k\omega_0^2/2$ is the diffraction length of the beam, τ ($= 19$ ps) is the pulse duration, and $k = 2\pi/\lambda$ is the wave vector, all in free space. I_{00} is the on-axis peak irradiance at the focus. Integration of Eq. (1) over t from $-\infty$ to ∞ and over the entire beam cross-section relates the pulse energy to I_{00} as $\varepsilon = I_{00}(\sqrt{\pi^3}\,\omega_0^2\tau)/2$. The irradiance and phase of each pulse in a dashed envelope shown in Fig. 2 are the same as those given by Eqs. (1) and (2), respectively, except I_{00} being modulated by the envelope function.

3. Results and discussion

Using single ps pulses with energy of $\varepsilon = 0.5$ μJ, we perform the Z-scan measurements on a C_{60}/toluene solution, prepared to have a concentration of 6.0×10^{17} cm^{-3} and contained in an 1 mm thick quartz cell. The results are shown in Fig. 1a: dots are obtained without aperture and crosses with an aperture (1.2 mm in radius) placed at a distance of 22 cm after the focus. Both curves are normalized to give a (linear) transmittance equal to one in the linear regimes, i.e., regions of large $|z|$. Division of the crosses by the dots yields the divided Z-scan curve shown by the crosses in Fig. 1b. Appearance of a valley on the $-z$ side and a peak on the $+z$ side is attributed to a positive lensing effect, which augments the beam divergence at the aperture when the sample is before the focus, and lessens the beam divergence when the sample is after the focus. Using the same procedure on the sample, after being diluted to one-tenth of its original concentration (i.e., 6.0×10^{16} cm^{-3}), a divided Z-scan curve with the full ns pulse envelopes at input energy $\varepsilon = 2.0$ μJ is obtained. As shown by the dots of Fig. 1b, this curve exhibits a peak on the $-z$ side and a valley on the $+z$ side, indicating a negative lensing effect.

To explain the experimental results, we use a five-energy-band model shown in Fig. 3 to interpret the optical excitation and subsequent relaxation. Each band (including the associated vibronic levels $|v\rangle$) is conventionally named as S_m for the singlet manifold or T_m for the triplet manifold, where the subscript m refers to the state formed from certain electronic configurations in molecular orbitals.

At thermal equilibrium, the unperturbed C_{60} molecules reside in the lowest electronic state S_0. Pumped by a laser pulse at 532 nm, the molecules are promoted via an one-photon process to a vibronic level of S_1, from which they relax to the zero-point level $|0\rangle$ of S_1 in a few ps [2], and then undergo one of the following three processes: (1) internal conversion (with a time constant of $\tau_{IC} = 30$ ns) to the bottom of S_0, (2) intersystem crossing (with a time constant of $\tau_{ISC} = 1.2$ ns) to T_1 [4], or (3) one-photon excitation to a vibronic level of S_2. Those ex-

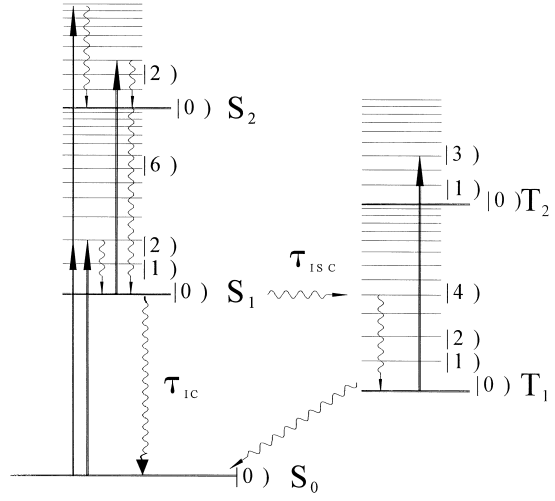

Fig. 3. The five energy-level diagram showing optical excitation (arrows), relaxations (wiggly lines). $|v\rangle$ refers to the vibrational eigenstates involved in the transitions.

cited to the vibronic levels of S_2 nonradiatively decay to a vibronic level of S_1 in subpicoseconds [2]. Those relaxing to T_1 can further be excited to T_2 if the pulse duration is comparable with τ_{ISC} or longer.

Accompanying each absorption (excitation) process mentioned above, there is instantaneous refraction according to the Kramer–Kronig relation. Following each relaxation, there is a temperature rise (ΔT) and thus an additional refractive index change $\Delta n_{\text{thermal}} = (\mathrm{d}n/\mathrm{d}t)\Delta T$ [5]. Since ΔT is larger around the beam axis than away from the axis for TEM_{00} mode laser excitation, the resultant nonuniform spatial distribution of $\Delta n_{\text{thermal}}$ produces a (thermal) lensing effect with either positive or negative sign depending on the sign of $(\mathrm{d}n/\mathrm{d}T)$. Since, as estimated below, a time of 299 ps is needed for C_{60}/toluene to reach local thermal equilibrium after an excitation, the thermal lensing effect is relevant only when pulses longer than hundreds of ps are used.

In this estimation we simply multiply the time for energy transfer between two adjacent solvent molecules by half the number of solvent molecules between two neighboring solute (antenna) molecules in order to arrive at the local thermal equilibrium time. The solvent–solvent time is taken to be the energy transfer time (13 ps) from an azulene (antenna) molecule to the surrounding methanol molecules, experimentally determined by Seilmeier and Kaiser [6]. A total of 46 toluene molecules between two neighboring C_{60} (antenna) is concluded because the solution we use has a concentration of 6.0×10^{16} cm^{-3} which implies an average nearest antenna–antenna separation of 2.6×10^{-6} cm. This is 46 times the molecular size of the solvent (0.87 g cm^{-3} and 92 g mol^{-1} for toluene).

In our investigation with 19 ps pulses, both the thermal lensing effect and the triplet transition are assumed irrelevant based on the thermal equilibrium time estimated above and the *n*s S_1 state lifetime. As a result, nonlinear absorption and refraction arise from transitions among the singlets alone and the equations governing the irradiance and phase changes, modified from Ref. [7], are

$$\frac{\mathrm{d}I}{\mathrm{d}z'} \equiv -\alpha I = -\left[(\sigma_a)_{S_0} N_{S_0} + (\sigma_a)_{S_1} N_{S_1}\right] I \qquad (3)$$

and

$$\frac{\mathrm{d}\phi}{\mathrm{d}z'} \equiv k\Delta n = (\sigma_r)_{S_0} N_{S_0} + (\sigma_r)_{S_1} N_{S_1} + kn_2 I. \qquad (4)$$

where I and ϕ represent the irradiance and phase, and z' the penetration depth. α and Δn denote the absorptive coefficient and change of refractive index. The first two terms on the right-hand sides of both equations pertain, in order, to the one-photon excitations $S_0 \rightarrow S_1$ and $S_1 \rightarrow S_2$. N represents the population density (number of C_{60} molecules per volume) of the state specified by the subscripts. n_2 in Eq. (4) is the Kerr nonlinear refractive coefficient of the solvent and its value of 5.5×10^{-15} cm^2 W^{-1} is adopted from Ref. [8]. For Eqs. (3) and (4), the associated population-change rates of the states involved are [7]

$$\frac{\mathrm{d}N_{S_0}}{\mathrm{d}t} = -\frac{(\sigma_a)_{S_0} N_{S_0} I}{\hbar\omega} \qquad (5)$$

and

$$\frac{\mathrm{d}N_{S_1}}{\mathrm{d}t} = \frac{(\sigma_a)_{S_0} N_{S_0} I}{\hbar\omega}, \qquad (6)$$

where the intraband relaxations and $S_2 \rightarrow S_1$ relaxation are assumed instantaneous.

Given the input irradiance I_0 and phase ϕ_0 (or equivalently the electric field E_0) at certain sample position z by Eqs. (1) and (2), and the initial population density $N_{S_0}(-\infty) = 6.0 \times 10^{17}$ cm^{-3}, we numerically integrate Eqs. (3)–(6) over the sample thickness L to obtain the irradiance I_L and phase ϕ_L (or the electric field E_L) at the exit surface. Using the Huygens–Fresnel propagation formalism [9], we deduce the irradiance at the aperture (I_a) from E_L. While integration of I_L over the pulse duration and beam cross-section gives an energy corresponding to that detected by D_2 without aperture, integration of I_a over the pulse duration and the aperture cross-section gives an energy corresponding to that detected by D_2 with an aperture. Repetition of the integration for all the sample z positions generates the theoretical Z-scan curves for fitting the experimental results. Using, $(\sigma_a)_{S_0} = 3.2 \times 10^{-18}$ cm^2, $(\sigma_a)_{S_1} = 1.5 \times 10^{-17}$ cm^2, $(\sigma_r)_{S_0} = 0$ cm^2, and $(\sigma_r)_{S_1} = 1.4 \times 10^{-17}$ cm^2, the best fits, shown by continuous-line curves in Fig. 1a,b, are obtained. Since substitution of the (σ_r)'s into Eq. (4) yields a positive Δn with its maximum on the beam axis, the nonlinear refraction

responsible for the positive lensing effect is associated with a positive sign.

When the full pulse envelopes are used, the thermal lensing effect and triplet state population come into play. This is qualitatively understandable. First, the pulse separation time of 7 ns among the ps pulses in the envelopes is much longer than the local thermal equilibrium time of 299 ps but much shorter than the ms order thermal diffusion time [1]. Secondly, it is longer than the intersystem crossing time of 1.2 ns. Thus, when an individual ps pulse in an envelope enters the sample, thermal lensing effect and triplet state population produced by earlier ps pulses will affect its irradiance and phase changes. The observed sign change of nonlinear refraction relative to that of single ps pulse excitation is thus attributed to thermal nonlinear refraction and electronic transitions among the triplet states. Quantitative study of these two processes requires calculations of the population accumulated on T_1, the temperature rise (ΔT) and temperature-rise-induced changes in solvent density and solute concentration for each ps pulse. The population calculation can be performed by simply introducing the intersystem crossing into the rate equation, whereas the knowledge of ΔT and subsequent changes in solvent density and solute concentration requires more understanding of intermolecular energy transfer process. This will be the subject of our future study.

Acknowledgements

The authors gratefully acknowledge financial supports from National Science Council of Taiwan for one of the authors (T.-H.W.) (NSC 88-2112-M-194-015 and NSC 89-2112-M-194-014) and one of the authors (T.-H.H.) (NSC 88-2112-M-194-008 and NSC 89-2112-M-194-007).

References

[1] M. Sheik-Bahae, A.A. Said, T.H. Wei, D.J. Hagan, E.W. Van Stryland, IEEE J. Quantum Electron. 26 (1990) 760.
[2] T.W. Ebbesen, K. Tanigaki, S. Kuroshima, Chem. Phys. Lett. 181 (1991) 501.
[3] A. Yariv, Optical Electronics, 4th edn., Saunders, Chicago, IL, 1991, p. 48.
[4] C. Li, L. Zhang, R. Wang, Y. Song, Y. Wang, J. Opt. Soc. Am. B 8 (1994) 1356.
[5] G.L. Wood, M.J. Miller, A.G. Mott, Opt. Lett. 20 (1995) 973.
[6] A. Seilmeier, W. Kaiser, in: W. Kaiser (Ed.), Ultrashort Laser Pulses, 2nd edn., Springer, Berlin, 1993, p. 305.
[7] T.H. Wei, T.H. Huang, M.S. Lin, Appl. Phys. Lett. 72 (1998) 2505.
[8] T.H. Wei, D.J. Hagan, M.J. Sence, E.W. Van Stryland, J.W. Perry, D.R. Coulter, Appl. Phys. B 54 (1992) 46.
[9] M. Born, E. Wolf, Principles of Optics, 5th edn., Pergamon, Oxford, 1975, p. 383.